

Effects of Coordination to a Macrocyclic Cobalt Complex on the Electrochemistry of Dioxygen, Superoxide, and Hydroperoxide

Chan Kang and Fred C. Anson*

Arthur Amos Noyes Laboratories,[†] Division of Chemistry and Chemical Engineering,
California Institute of Technology, Pasadena, California 91125

Received November 30, 1994[⊗]

The reduction of O₂ as catalyzed by the complex of Co(II) with the macrocyclic ligand *C-meso*-5,7,7,12,14,14-hexamethyl-1,4,8,11-tetraazacyclotetradecane (hmc) was examined using electrochemical techniques. The metastable (hmc)CoOO²⁺ complex is an intermediate in the catalytic cycle. It is in rapid equilibrium with O₂ and (hmc)Co²⁺. The (hmc)CoOO²⁺ complex is a strong oxidant that is rapidly reduced to (hmc)CoOOH²⁺ at the potential where (hmc)Co³⁺ is reduced to (hmc)Co²⁺ (0.38 V vs NHE). At more negative potentials (0.07 V) (hmc)CoOOH²⁺ is reduced irreversibly to H₂O₂ and (hmc)Co²⁺ and the catalytic electroreduction of O₂ to H₂O₂ ensues. The electroreduction of (coordinated) O₂ to (coordinated) OOH⁻ at potentials where uncoordinated O₂ is not reducible is attributed to stabilization of the reduced ligand by the cobalt center to which it is coordinated. Digital simulation was employed to obtain an estimate (0.99 V vs NHE) for the formal potential of the (hmc)CoOO²⁺/(hmc)CoOOH²⁺ couple at pH 1. The OOH⁻ ligand coordinated to (hmc)Co³⁺ is electrooxidized to O₂ near 0.9 V vs NHE, but uncoordinated H₂O₂ is unreactive at this potential. The affinities of OO⁻ and OOH⁻ for (hmc)Co³⁺ are comparable despite their highly disparate Bronsted basicities. Greater stabilization of the (hmc)CoOO²⁺ than of the (hmc)CoOOH²⁺ complex by LMCT is suggested to account for this result.

The effect of coordination to transition metal centers on the electrochemical reactivity of O₂ (and H₂O₂) is a subject of continuing interest.¹ The factors responsible for the catalytic activity of transition metal complexes in the reduction or electroreduction of O₂ are not well understood, and comparisons of the behaviors of chemically similar complexes are desirable to establish a basis from which more satisfying mechanistic accounts may be derived. In this spirit we have examined the electrochemistry of O₂ in the presence of a variety of complexes of cobalt,² iron,³ copper,⁴ and chromium.⁵ In a previous study of the effect of O₂ on the electrochemistry of the cobalt(II) complex of 1,4,8,11-tetraazacyclotetradecane (cyclam) the behavior observed was complex because both a mononuclear superoxide complex and a binuclear μ -peroxo complex were formed.² This difficulty was avoided in the present study by employing *C-meso*-5,7,7,12,14,14-hexamethyl-1,4,8,11-tetraazacyclotetradecane (hmc) in place of cyclam to prepare complexes with Co(II) and Co(III). Espenson and co-workers⁶ have shown that the steric crowding produced by the six methyl groups essentially prevents the formation of a μ -peroxo dinuclear complex during the oxidation of the cobalt(II) complex with O₂, which simplified the interpretation of the observed electrochemical responses. Voltammetric waves were obtained that could be assigned to the reduction of the (hmc)CoOO²⁺ complex to (hmc)CoOOH²⁺ followed by the reduction of the latter complex to (hmc)Co(OH₂)²⁺ and H₂O₂. Estimates of the formal

potentials for these two electrode reactions were obtained, and some aspects of the electrochemical reactivities of the coordinated ligands are discussed.

Experimental Section

Materials. Reagent grade chemicals were used as received from commercial sources: Ru(NH₃)₆Cl₃ (Strem Chemical Co.), H₂O₂ (30%) and CF₃COOH (E & M Chemical Co.), CF₃SO₃H (Aldrich Chemical Co). The macrocyclic ligand *C-meso*-5,7,7,12,14,14-hexamethyl-1,4,8,11-tetraazacyclotetradecane (hmc) and [(hmc)Co](CF₃SO₃)₂ were synthesized according to procedures described in the literature.^{6–8} The pale red [(hmc)Co](CF₃SO₃)₂ was stored under argon in a refrigerator to avoid the gradual changes that occurred when it was exposed to air. Solutions were prepared from laboratory deionized water that was further purified by passage through a purification train (Milli-Q, Millipore Co.). The (hmc)Co³⁺ complex was prepared in solution by electrolytic oxidation of (hmc)Co²⁺ in the absence of O₂. Solutions of (hmc)CoOO²⁺ were prepared by adding small aliquots of a concentrated solution of (hmc)Co²⁺ to O₂-saturated solutions. Solutions of (hmc)CoOOH²⁺ were prepared by adding 1 equiv of Ru(NH₃)₆²⁺ to solutions of (hmc)CoOO²⁺ immediately after their preparation (without removal of the excess O₂ present). Ru(NH₃)₆²⁺ was prepared by reduction of Ru(NH₃)₆³⁺ with amalgamated zinc. The concentrations of O₂ in test solutions were controlled by means of a calibrated gas-mixing valve.

Apparatus and Procedures. The conventional electrochemical cell employed has been described.⁵ The working electrodes were a glassy carbon disk–glassy carbon ring electrode or a glassy carbon disk–platinum ring electrode (Pine Instrument Co.). The dimensions of the electrodes were $r_1 = 0.281$ cm, $r_2 = 0.312$ cm, $r_3 = 0.396$ cm and $r_1 = 0.229$ cm, $r_2 = 0.246$ cm, $r_3 = 0.269$ cm, respectively, where r_1 is the radius of the disk and r_2 and r_3 are the inner and outer radii of the ring. The collection efficiencies⁹ measured with the Fe(CN)₆^{3-/4-} couple were in good agreement with those calculated from the dimensions of the disks and ring electrodes. In experiments where

* Contribution No. 9025.

[⊗] Abstract published in *Advance ACS Abstracts*, April 15, 1995.

- (1) (a) *Chem. Rev.* **1994**, *94*, 567–856. (b) Fukuzumi, S.; Mochizuki, S.; Tanaka, T. *Inorg. Chem.* **1989**, *28*, 2459. (c) Maeder, M.; Mäcke, H. R. *Inorg. Chem.* **1994**, *33*, 3135.
- (2) Geiger, T.; Anson, F. C. *J. Am. Chem. Soc.* **1981**, *103*, 7489.
- (3) Shi, C.; Anson, F. C. *Inorg. Chem.* **1990**, *29*, 4298.
- (4) (a) Zhang, J.; Anson, F. C. *J. Electroanal. Chem. Interfacial Electrochem.* **1992**, *341*, 323. (b) Zhang, J.; Anson, F. C. *J. Electroanal. Chem. Interfacial Electrochem.* **1993**, *348*, 81. (c) Lei, Y.; Anson, F. C. *Inorg. Chem.* **1995**, *34*, 1083.
- (5) Kang, C.; Anson, F. C. *Inorg. Chem.* **1994**, *33*, 2624.
- (6) Bakac, A.; Espenson, J. H. *J. Am. Chem. Soc.* **1990**, *112*, 2273.

(7) Hay, R. W.; Lawrance, G. A.; Cutis, N. F. *J. Chem. Soc., Perkin Trans. I* **1975**, 591.

(8) Rillema, D. P.; Endicott, J. F.; Papaconstantinou, E. *Inorg. Chem.* **1971**, *10*, 1739.

(9) Bard, A. J.; Faulkner, L. R. *Electrochemical Methods*; John Wiley and Sons: New York, 1980; p 302.

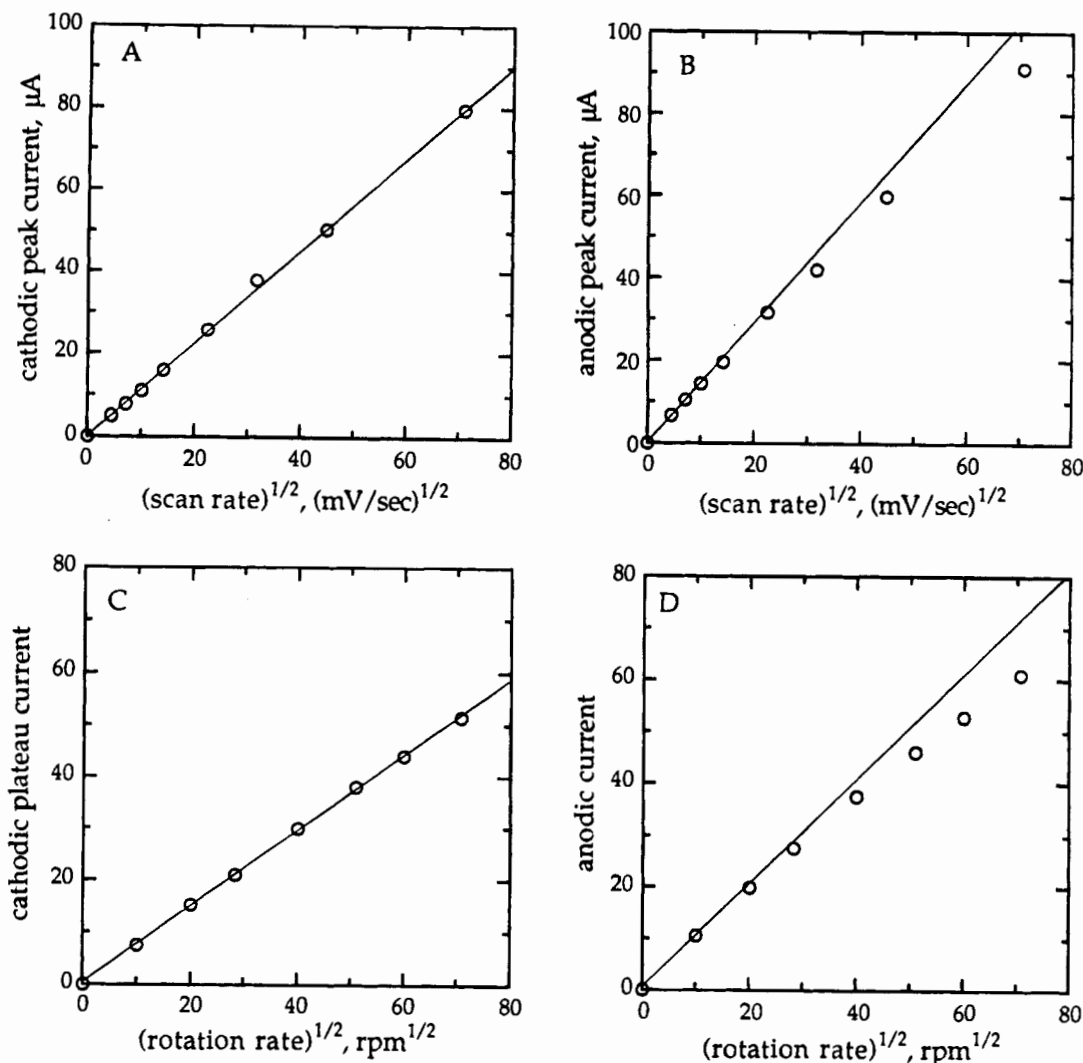


Figure 1. (A, B) Randles–Sevcik plots of voltammetric peak currents vs $(\text{scan rate})^{1/2}$ and (C, D) Levich plots of rotating disk plateau currents vs $(\text{rotation rate})^{1/2}$ for (A, C) reduction of 0.31 mM $(\text{hmc})\text{Co}^{3+}$ and (B, D) oxidation of 0.42 mM $(\text{hmc})\text{Co}^{2+}$. The currents plotted in part D are the observed currents at 0.6 V. Conditions: glassy carbon electrode ($A = 0.248 \text{ cm}^2$); supporting electrolyte 0.1 M CF_3COOH .

the ring electrodes were not involved, they were disconnected from the potentiostat. The glassy carbon electrodes were polished with 0.3 μm alumina followed by sonication in pure water before each experiment. No oxidative activation of the glassy carbon was employed¹⁰ because attempts to do so produced less reproducible voltammetric responses, especially during the electrooxidation of $(\text{hmc})\text{Co}^{2+}$.

Conventional electrochemical instrumentation was employed. Spectra were recorded with a Hewlett-Packard Model 8450 spectrophotometer. Digital simulations were performed using the Digisim 1.0 software package (BAS, Inc.). All experiments were conducted in 0.1 M CF_3COOH as supporting electrolyte. Parameters employed in the calculation of Levich currents for the reduction of O_2 : kinematic viscosity of water, $0.01 \text{ cm}^2 \text{ s}^{-1}$; $[\text{O}_2]$ in air-saturated solutions, 0.25 mM; diffusion coefficient of O_2 , $1.8 \times 10^{-5} \text{ cm}^2 \text{ s}^{-1}$. Potentials were measured and are quoted with respect to a Ag/AgCl (3M NaCl) reference electrode whose potential is 0.22 V vs NHE. Experiments were conducted at the ambient laboratory temperature ($22 \pm 2 \text{ }^\circ\text{C}$).

Results

Electrochemical Responses of $(\text{hmc})\text{Co}^{2+}$ and $(\text{hmc})\text{Co}^{3+}$.

Cyclic voltammograms and rotating disk current–potential curves were recorded with solutions of $(\text{hmc})\text{Co}^{2+}$ or (hmc)

Co^{3+} . (The coordination spheres of the cobalt centers are presumed to be completed by water molecules that will not be shown.) Both the oxidation of $(\text{hmc})\text{Co}^{2+}$ and the reduction of $(\text{hmc})\text{Co}^{3+}$ exhibit simple, diffusion-controlled responses at low current densities as reflected in the initially linear Randles–Sevcik¹¹ (Figure 1A,B) and Levich¹² plots (Figure 1C,D). However, as was also observed with the corresponding cobalt cyclam complex,² the oxidation of $(\text{hmc})\text{Co}^{2+}$ deviates from pure diffusion control at higher scan rates (Figure 1B) or electrode rotation rates (Figure 1D). The deviations can be diminished by oxidative activation of the glassy carbon electrode,¹⁰ but we elected not to utilize such a procedure because better reproducibility was obtained at electrodes that were polished with alumina but not oxidized. The reduction of $(\text{hmc})\text{Co}^{3+}$ remained diffusion-controlled throughout the range of scan and rotation rates investigated (Figure 1A,C). The contrast in the behaviors of the Co(II) and Co(III) complexes suggests that the coordination of a suitable axial ligand to the Co(II) center may be required to facilitate its oxidation, perhaps by an inner-sphere mechanism. If the needed ligand were provided by one of the functional groups generated on the glassy carbon electrode

(11) (a) Randles, J. E. B. *Trans. Faraday Soc.* **1948**, *44*, 327. (b) Sevcik, A. *Collect. Czech. Chem. Commun.* **1948**, *13*, 349.

(12) Levich, V. G. *Physicochemical Hydrodynamics*; Prentice-Hall: Englewood Cliffs, NJ, 1962.

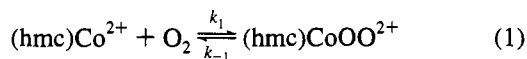
(10) Cabaniss, G. E.; Diamantis, A. A.; Murphy, W. R., Jr.; Linton, R. W.; Meyer, T. J. *J. Am. Chem. Soc.*, **1985**, *107*, 1845.

surface by electrooxidation, the sensitivity of the oxidation of (hmc)Co²⁺ to the pretreatment of the electrode surface would be understandable.

The formal potential of the (hmc)Co^{3+/2+} couple obtained from the average of the peak potentials for a voltammogram recorded at 20 mV s⁻¹ was 0.16 V vs Ag/AgCl in 0.1 M CF₃COOH. This value is considerably smaller than the value (0.37 V vs Ag/AgCl) reported from rather involved potentiometric measurements with 1 M HClO₄ as supporting electrolyte¹³ and somewhat smaller than the value (0.27 V vs Ag/AgCl) obtained from cyclic voltammetry using a mercury electrode in 0.1 M HClO₄.¹⁴ We confirmed this value using a glassy carbon electrode in the same electrolyte. The rather large variation in the reported formal potentials reflects an unusual sensitivity of the (hmc)Co^{3+/2+} couple to the nature and concentration of the supporting electrolytes. All of the experiments in the present study were conducted in 0.1 M CF₃COOH, in which the formal potential of 0.16 V applies.

The diffusion coefficients of (hmc)Co³⁺ and (hmc)Co²⁺ were evaluated from the initial linear portions of the plots in Figure 1C,D. A value of 3.9×10^{-6} cm² s⁻¹ was obtained for both complexes.

Reduction of (hmc)Co³⁺ in the Presence of O₂. The previous work of Endicott and co-workers¹³ and of Bakac and Espenson⁶ has provided a thorough account of the kinetics and thermodynamics governing the reaction of (hmc)Co²⁺ with O₂, reaction 1. The reaction is rapid, $k_1 = 5 \times 10^6$ M⁻¹ s⁻¹,⁶ but



far from quantitative, $K_1 = k_1/k_{-1} = 3 \times 10^2$ M⁻¹.⁶ The occurrence of reaction 1 in the diffusion layer at electrode surfaces would be anticipated to produce significant effects when the voltammetric reduction of (hmc)Co³⁺ is carried out in the presence of O₂. The voltammetric behavior of mixtures of (hmc)Co³⁺ and O₂ was examined with a rotating glassy carbon ring–glassy carbon disk electrode, and the results are shown in Figure 2. Curve 1 resulted from the reduction of the (hmc)Co³⁺ complex at the disk electrode in the absence of O₂. The corresponding ring current–disk potential response is shown in curve 6. The ring electrode was held at 0.6 V, where the (hmc)Co²⁺ complex, produced at the disk and swept to the ring by the rotation of the electrode, was reoxidized to (hmc)Co³⁺. The ratio of the ring to the disk current on the plateaus of curves 1 and 6, i.e., the collection efficiency, was about 75% of the value obtained when the same measurement was carried out using the Fe(CN)₆^{3-/4-} or Ru(NH₃)₆^{3+/2+} redox couple. The implication of this result is that, even in the absence of O₂, not all of the (hmc)Co²⁺ complex generated at the disk is rapidly reoxidizable at the ring electrode at 0.6 V. As was shown in Figure 1D, Levich plots for the oxidation of (hmc)Co²⁺ are linear with slopes that match those for the reduction of (hmc)Co³⁺ up to current densities that are much greater than those corresponding to the ring currents in curve 6 of Figure 2. The low collection efficiencies for the oxidation of (hmc)Co²⁺ at the ring electrode and the nonlinearity in Levich plots for the oxidation of this complex at the disk electrode surely have a common origin which, however, remains to be identified. Nevertheless, the collection efficiencies obtained at carefully polished electrodes were quite reproducible, and it proved possible to utilize the ring–disk voltammetric responses to follow the interactions of (hmc)Co²⁺ with O₂ despite the lack of theoretical collection efficiencies in the absence of O₂.

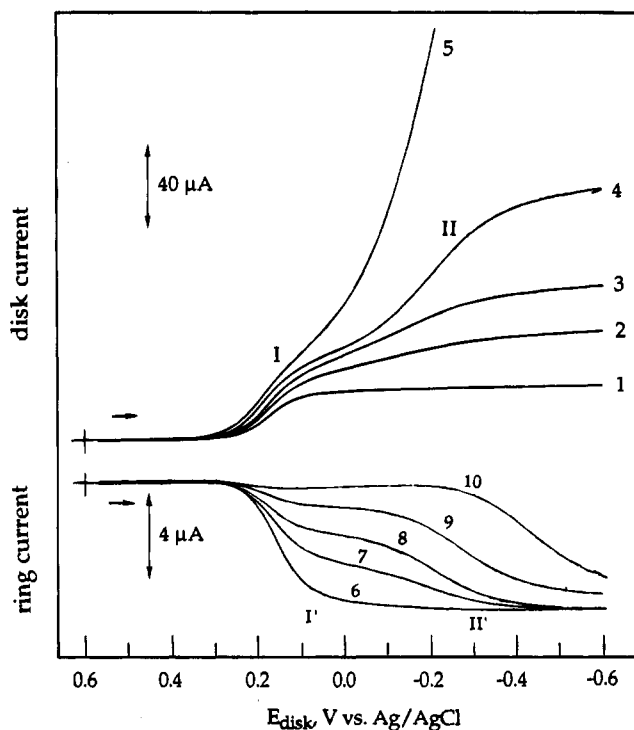


Figure 2. Current–potential curves recorded with a rotating ring–disk electrode in mixtures of 0.31 mM (hmc)Co³⁺ with O₂. Concentrations of O₂: (1, 6) 0, (2, 7) 0.06, (3, 8) 0.11, (4, 9) 0.25, (5, 10) 1.25 mM. The potential of the ring electrode was 0.6 V. Electrode rotation rate = 800 rpm. Scan rate = 10 mV s⁻¹. Supporting electrolyte: 0.1 M CF₃COOH.

Curves 2–5 in Figure 2 show the current–potential curves obtained at the disk electrode when increasing concentrations of O₂ were added to the solution used to record curve 1. There are several revealing features in these curves:

In the presence of O₂, two reduction waves are present. The first wave, labeled I in Figure 2, has a half-wave potential a little more positive than the only wave in curve 1 and a plateau current which increases with the concentration of O₂. The estimated magnitude of the plateau current of wave I is approximately twice as large as that in curve 1 at the two highest concentrations of O₂. A second reduction wave, labeled II in Figure 2, with a half-wave potential near –0.15 V is also present. This wave does not arise from the direct reduction of O₂ at the disk electrode which requires more negative potentials. The magnitude of wave II increases with the concentration of O₂, which causes it to overlap with wave I at higher concentrations of O₂.

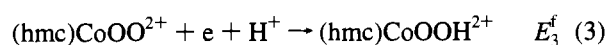
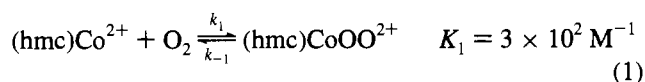
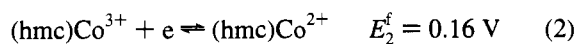
Curves 6–10 in Figure 2 show the responses obtained at the ring electrode (with its potential set at 0.6 V to oxidize the (hmc)Co²⁺ that reaches it) during the recording of curves 1–5 at the disk electrode. The known thermodynamic and kinetic characteristics of reaction 1⁶ provide a basis for a reasonable interpretation of the ring currents shown in Figure 2: Less of the (hmc)Co²⁺ generated at the disk electrode at wave I reaches the ring electrode when O₂ is present in the solution (note the diminished magnitude of wave I' in curves 7–10) because much of it is consumed in reaction 1. At the highest concentration of O₂ (1.25 mM), curve 10 in Figure 2 shows that almost all of the (hmc)Co²⁺ generated at the disk is consumed before it can reach the ring to be oxidized. However, reaction 1 is rapidly reversible so that an additional reaction is required to explain the diminishment in the quantities of oxidizable (hmc)Co²⁺ that arrive at the ring electrode in the presence of O₂. As will be shown, the additional step is the rapid and irreversible further

(13) Liteplo, M. P.; Endicott, J. F. *Inorg. Chem.* **1971**, *10*, 1420.

(14) Heckman, R. A.; Espenson, J. H. *Inorg. Chem.* **1979**, *18*, 38.

electroreduction of CoOO^{2+} to CoOOH^{2+} at the disk electrode. The equilibrium constant of reaction 1 corresponds to the conversion of only about 27% of the $(\text{hmc})\text{Co}^{2+}$ into $(\text{hmc})\text{CoOO}^{2+}$ at equilibrium in the 1.25 mM solution of O_2 . However, much more than 27% of the $(\text{hmc})\text{Co}^{2+}$ is consumed because reaction 1 is driven to the right by the removal of the $(\text{hmc})\text{CoOO}^{2+}$ complex through its further reduction to CoOOH^{2+} at the disk electrode. This further reduction is also responsible for the increases in the plateau currents at the disk electrode at wave I of curves 2–5 of Figure 2. The processes responsible for wave I in Figure 2 are shown in Scheme 1. As elaborated

Scheme 1



previously,² one factor that controls the total number of electrons consumed in wave I is the relative fluxes of O_2 and $(\text{hmc})\text{Co}^{3+}$ at the surface of the rotating disk electrode. The fluxes are proportional to each reactant's bulk concentration and (diffusion coefficient)^{2/3}. The larger diffusion coefficient of O_2 ($1.8 \times 10^{-5} \text{ cm}^2 \text{ s}^{-1}$) compared with $(\text{hmc})\text{Co}^{3+}$ ($3.9 \times 10^{-6} \text{ cm}^2 \text{ s}^{-1}$) causes the fluxes of O_2 and $(\text{hmc})\text{Co}^{3+}$ to become equal when the ratio of their concentrations is 0.36. Thus, the flux of $(\text{hmc})\text{Co}^{3+}$ exceeds that of O_2 for curve 2 of Figure 2, the converse is true for curves 4 and 5, and the two fluxes are essentially equal for curve 3. However, despite the availability of adequate O_2 for the stoichiometry shown in Scheme 1 to be realized with the solution used to record curve 3, somewhat fewer than two electrons per $(\text{hmc})\text{Co}^{3+}$ complex are actually consumed because the plateau current of wave I of curve 3 is less than twice as large as that of curve 1. The reason is that the relatively small value of K_1 prevents the conversion of more than a fraction of the $(\text{hmc})\text{Co}^{2+}$ to $(\text{hmc})\text{CoOO}^{2+}$. The further reduction of the $(\text{hmc})\text{CoOO}^{2+}$ that is formed causes additional $(\text{hmc})\text{Co}^{2+}$ to be consumed within the Levich layer at the surface of the disk, but some of the $(\text{hmc})\text{Co}^{2+}$ is swept from the layer without reacting with O_2 . This unreacted $(\text{hmc})\text{Co}^{2+}$ is responsible for wave I' in the ring current responses of curves 7–10 in Figure 2.

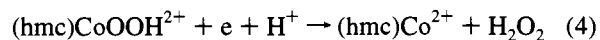
In solutions saturated with O_2 (curve 5 of Figure 2) the magnitude of wave I becomes approximately twice as large as that of curve 1 and almost no $(\text{hmc})\text{Co}^{2+}$ is detected at the ring (curve 10) as expected if the reactions of Scheme 1 all proceeded quantitatively.

It is noteworthy that, even at the low ratio of $[\text{O}_2]$ to $[(\text{hmc})\text{Co}^{3+}]$ used to record curve 2 in Figure 2, the plateau current of wave I is significantly larger than that in the absence of O_2 . If a μ -peroxo complex were formed under these conditions, as it is in corresponding experiments with $\text{Co}(\text{cyclam})$,² there would be no increase in the magnitude of the first wave. This lack of rapid formation of a μ -peroxo complex, even when the $(\text{hmc})\text{Co}^{2+}$ complex is present in excess of O_2 , is in accord with the observations of Bakac and Espenson.⁶

The use of Scheme 1 to account for the magnitude of wave I in Figure 2 implies that the formal potential of half-reaction 3 is more positive than that of half-reaction 2. We will return to this point in what follows and provide an estimate of E_3^f .

Wave II of curves 2–5 in Figure 2 has a plateau current which increases continuously with the concentration of O_2 rather than

reaching a limit in the way that wave I does. At concentrations of O_2 above about 0.06 mM, the plateau current of wave II corresponds to many more than two electrons per $(\text{hmc})\text{Co}^{3+}$ complex. Wave II originates in the half-reaction



The $(\text{hmc})\text{Co}^{2+}$ produced in half-reaction 4 reacts with any excess O_2 present (reaction 1), and the resulting $(\text{hmc})\text{CoOO}^{2+}$ is reduced via half-reactions 3 and 4 so that the $(\text{hmc})\text{Co}^{3+/2+}$ -catalyzed reduction of O_2 to H_2O_2 ensues on the plateau of wave II. This interpretation is confirmed by the ring current responses shown in curves 7–10: The increased anodic ring current (wave II') that results when the disk potential is scanned over wave II arises from the increased flux of $(\text{hmc})\text{Co}^{2+}$ that reaches the ring because both $(\text{hmc})\text{CoOO}^{2+}$ and $(\text{hmc})\text{CoOOH}^{2+}$ are reduced to $(\text{hmc})\text{Co}^{2+}$ and H_2O_2 at disk electrode potentials negative of -0.15 V . (H_2O_2 is not oxidized at the glassy carbon ring electrode at potentials less positive than $\sim 1.2 \text{ V}$.) With the lower concentrations of O_2 (curves 7 and 8), the ring currents increase to the values obtained in the absence of O_2 (curve 6) showing that all of the $(\text{hmc})\text{Co}^{2+}$ generated at the disk reaches the ring because essentially all of the O_2 in the Levich layer has been removed by means of Scheme 1 plus half-reaction 4. At higher concentrations of O_2 (curves 9 and 10), its catalyzed reduction is incomplete and some O_2 remains in the Levich layer to intercept some of the $(\text{hmc})\text{Co}^{2+}$ leaving the disk before it can reach the ring to be oxidized and smaller anodic ring currents are obtained.

Electrooxidation of $(\text{hmc})\text{CoOOH}^{2+}$. The proposed generation of the hydroperoxide complex of $(\text{hmc})\text{Co}^{3+}$ by reduction of $(\text{hmc})\text{Co}^{3+}$ in the presence of O_2 was based on analogy with the behavior of $\text{Co}(\text{cyclam})^{3+}$ and on the ring-disk voltammetry of Figure 2. The proposed reduction of the cobalt(III) center in the $(\text{hmc})\text{CoOOH}^{2+}$ complex at wave II in Figure 2 (half-reaction 4) explains the observed catalyzed reduction of O_2 to H_2O_2 . It was also of interest to inspect the possible electrooxidation of the hydroperoxide complex. A convenient method for doing so is shown in Figure 3, where the potential of the ring electrode was scanned while the potential of the disk electrode was held constant. With the disk potential maintained at 0.0 V in a solution containing 0.31 mM $(\text{hmc})\text{Co}^{3+}$ and 0.25 mM O_2 , i.e., at a potential on the plateau of wave I of curve 4 in Figure 2, the products generated at the disk are $(\text{hmc})\text{CoOOH}^{2+}$ and $(\text{hmc})\text{Co}^{2+}$ (Scheme 1) so the ring electrode is exposed to both complexes. Curve 1 of Figure 3 shows the ring current vs ring potential curve that resulted during this experiment. At ring potentials less positive than 0.2 V, there is cathodic ring current arising from reduction of $(\text{hmc})\text{Co}^{3+}$ at the ring. At potentials between ca. 0.35 and 0.8 V, there is a steady anodic ring current arising from the oxidation of $(\text{hmc})\text{Co}^{2+}$ that reaches the ring. At potentials positive of 0.8 V, large additional ring current flows that must arise from the oxidation of $(\text{hmc})\text{CoOOH}^{2+}$ because no other component of the solution is oxidized at glassy carbon at these potentials. The current response extends over a range of potentials and runs into the anodic background for the ring electrode before a plateau is reached. The electrooxidation of $(\text{hmc})\text{CoOOH}^{2+}$ is presumed to be a two-electron process with $(\text{hmc})\text{Co}^{3+}$ and O_2 as the oxidation products because any $(\text{hmc})\text{CoOO}^{2+}$ formed as an intermediate would be rapidly oxidized to produce the same products.

When the same experiment was repeated with the disk electrode potential maintained at -0.5 V instead of 0.0 V, the ring current response shown in curve 2 of Figure 3 was obtained. Only the oxidation of $(\text{hmc})\text{Co}^{2+}$ is observed at the ring because

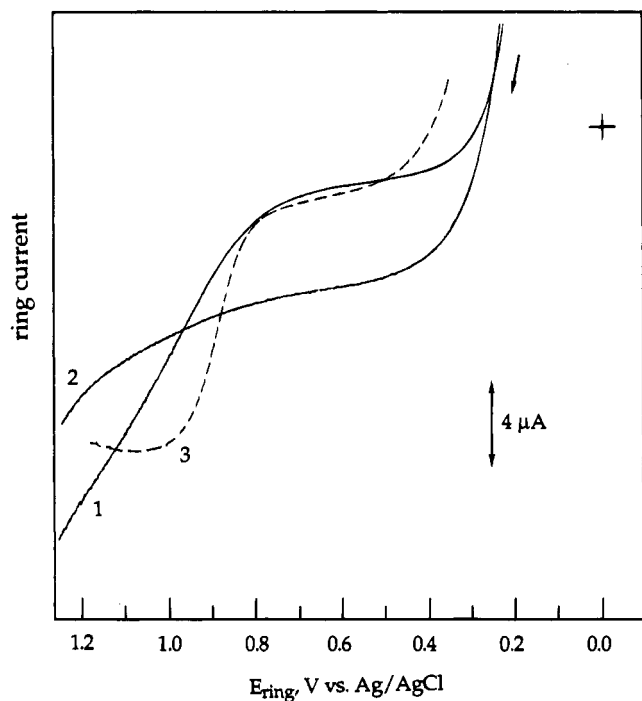


Figure 3. Ring current vs ring potential curves with constant disk potentials in a 0.31 mM solution of $(hmc)Co^{3+}$ saturated with air (0.25 mM O₂): (1) disk potential at 0.0 V, glassy carbon ring; (2) disk potential at -0.5 V, glassy carbon ring; (3) disk potential at -0.5 V, platinum ring. Other conditions were as in Figure 2.

at a disk potential of -0.5 V $(hmc)CoOOH^{2+}$ is reduced at the disk to $(hmc)Co^{2+}$ and H₂O₂. When this experiment was repeated using a platinum ring electrode in place of the glassy carbon ring, the response shown in curve 3 was obtained. Now the oxidation of $(hmc)Co^{2+}$ at the ring is followed by a large oxidation wave at 0.9 V, where H₂O₂ is oxidized at Pt. The current for the oxidation of H₂O₂ is larger than that for the oxidation of $(hmc)Co^{2+}$ both because the oxidation of H₂O₂ involves twice as many electrons and because some of the $(hmc)Co^{2+}$ generated at the disk is consumed by reaction with residual O₂ before it reaches the ring (Figure 2, curves 4 and 9).

The oxidizability of $(hmc)CoOOH^{2+}$ but not H₂O₂ at the glassy carbon ring produced an interesting set of ring current responses at ring potentials more positive than the 0.6 V used in Figure 2. In Figure 4 the ring currents are shown for ring potentials of 0.9, 1.0, and 1.2 V as the disk potential was scanned over the waves for the reduction of $(hmc)Co^{3+}$ in the presence of O₂. At a ring potential of 0.9 V, the $(hmc)CoOOH^{2+}$ complex formed at the disk at wave I contributes rather little to the ring current at wave I' so the response resembles curve 9 in Figure 2. At a ring potential of 1.0 and, especially, at 1.2 V, much larger ring currents are obtained because the two-electron oxidation of $(hmc)CoOOH^{2+}$ proceeds along with the oxidation of $(hmc)Co^{2+}$. The ring current passes through a maximum and decreases as the disk is scanned over wave II because H₂O₂ instead of $(hmc)CoOOH^{2+}$ is then produced at the disk and the H₂O₂ is not oxidizable at the glassy carbon ring.

A summary of the half-reactions that have been assigned to the disk and ring responses in Figure 2 is given in Table 1.

Electrochemistry of $(hmc)CoOO^{2+}$. The $(hmc)CoOO^{2+}$ complex cannot be prepared electrochemically by reducing $(hmc)Co^{3+}$ in the presence of O₂ because $(hmc)CoOO^{2+}$ is reduced to $(hmc)CoOOH^{2+}$ at the potentials required for the reduction of $(hmc)Co^{3+}$. However, the complex can be prepared by reacting $(hmc)Co^{2+}$ with O₂ in solution.⁶ The complex

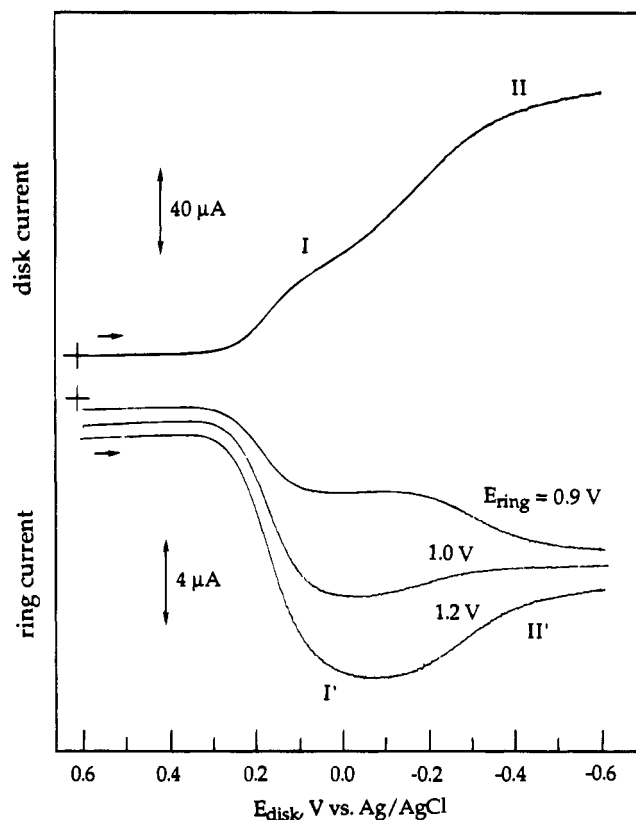


Figure 4. Current-potential curves recorded at a rotating glassy carbon disk-glassy carbon ring electrode with the solution from Figure 3. The potentials of the ring electrode are indicated.

Table 1. Half-Reactions Corresponding to the Currents at the Disk and Ring Electrodes in Figure 2

curve no. (electrode)	wave	half-reaction(s)
1 (disk)	I	$(hmc)Co^{3+} + e \rightleftharpoons (hmc)Co^{2+}$
6 (ring)	I'	$(hmc)Co^{2+} - e \rightleftharpoons (hmc)Co^{3+}$
2-4 (disk)	I	$(hmc)Co^{3+} + e \rightleftharpoons (hmc)Co^{2+}$
5 (disk)	I	$(hmc)Co^{3+} + O_2 + H^+ + 2e \rightarrow (hmc)CoOOH^{2+}$ $(hmc)Co^{3+} + O_2 + H^+ + 2e \rightarrow (hmc)CoOOH^{2+}$
2-5 (disk)	II	$(hmc)Co^{3+} + O_2 + 3e + 2H^+ \xrightarrow[cat.]{(hmc)Co^{3+/2+}} H_2O_2 + (hmc)Co^{2+}$
7-10 (ring)	I' and II'	$(hmc)Co^{2+} - e \rightleftharpoons (hmc)Co^{3+}$

decomposes spontaneously,¹⁵ but its lifetime is adequate to allow its electrochemistry to be observed. In Figure 5 are shown rotating disk voltammograms recorded in a solution prepared by adding 0.4 mmol/L of $(hmc)Co^{2+}$ to a solution saturated with O₂. The response obtained 1 min after the reactants were mixed consists of a single, composite wave with both an anodic and a cathodic current plateau. The anodic current decreases to zero in about 10 min while the cathodic current increases somewhat. The response shown after 10 min in Figure 5 is similar to that obtained when the same quantity of $(hmc)Co^{3+}$ was added to the O₂-saturated solution. The decrease in the anodic current reflects the slow irreversible oxidation of $(hmc)Co^{2+}$ to a mixture of products as described by Bakac and Espenson.^{6,15} The magnitudes of the anodic plateau currents in the curves of Figure 5 reflect the sum of the $(hmc)Co^{2+}$ and $(hmc)CoOO^{2+}$ complexes that remain in the solution at each time because these two complexes are in rapid equilibrium.

The cathodic plateau current results from the reduction of $(hmc)CoOO^{2+}$ to $(hmc)CoOOH^{2+}$ plus the reduction of any

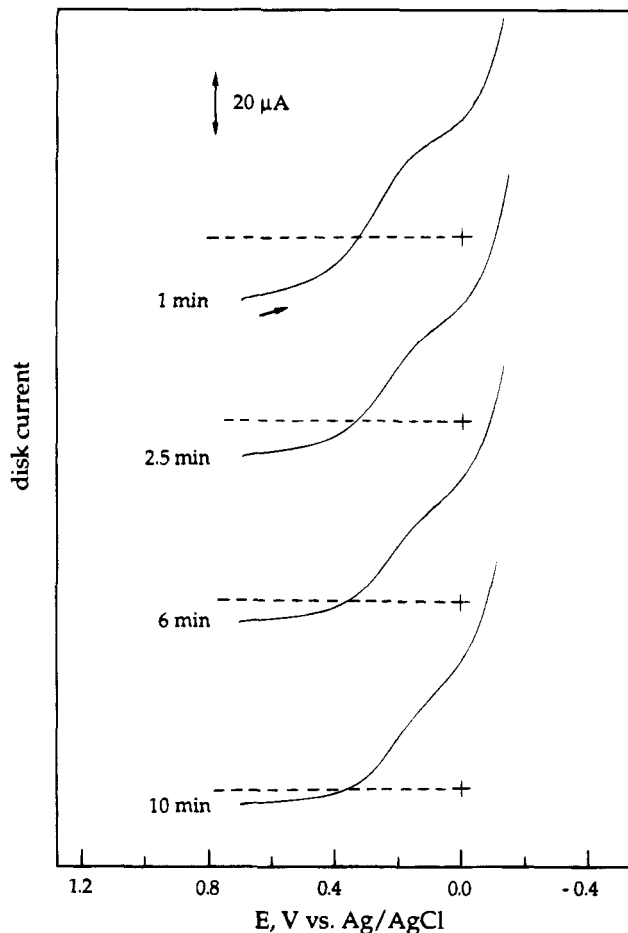


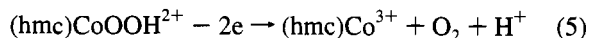
Figure 5. Current-potential curves recorded with the rotating disk electrode in a solution prepared by adding 0.4 mmol/L of $(hmc)Co^{2+}$ to a solution saturated with O_2 . The times elapsed since the mixture was prepared are indicated. Other conditions were as in Figure 2.

$(hmc)Co^{3+}$ produced by the chemical oxidation of $(hmc)Co^{2+}$ by O_2 . Before the chemical oxidation of $(hmc)Co^{2+}$ becomes significant, one would expect equal cathodic and anodic plateau currents because both overall electrode processes involve one electron per cobalt center. In fact, the cathodic plateau current recorded 1 min after the reactants were mixed is somewhat larger than the anodic current which is the expected result if partial chemical oxidation of $(hmc)Co^{2+}$ to $(hmc)Co^{3+}$ had occurred during the first minute after mixing. After 10 min, the cathodic wave resembles those in Figure 2 and represents the reduction of $(hmc)Co^{3+}$ in the presence of O_2 to yield $(hmc)CoOOH^{2+}$. If none of the $(hmc)Co^{2+}$ initially added to the solution had been consumed in irreversible side reactions, the final cathodic plateau current would be expected to be 2 times as large as the initial cathodic current because two electrons are required to reduce $(hmc)Co^{3+}$ to $(hmc)CoOOH^{2+}$ in the presence of excess O_2 while only one electron is needed to produce the same product from a mixture of $(hmc)Co^{2+}$ and O_2 . The fact that the final cathodic plateau current actually becomes slightly smaller than the initial current shows that a substantial portion of the $(hmc)Co^{2+}$ is converted to products other than $(hmc)Co^{3+}$ and that these products are not reduced on the cathodic plateau. The presence of such products after reaction times of several minutes was also reported by Bakac and Espenson.⁶

The potential where the composite voltammogram recorded after 1 min in Figure 5 crosses the zero-current axis is a "mixed potential" where the rates of the oxidation of $(hmc)Co^{2+}$ and the reduction of $(hmc)CoOO^{2+}$ are equal. The observed value of 0.35 V is a lower limit for the formal potential of the (hmc) -

$CoOO^{2+}/(hmc)CoOOH^{2+}$ couple, but the actual value is much more positive, as will be demonstrated in what follows.

Electrochemistry of $(hmc)CoOOH^{2+}$. Moderately stable solutions of $(hmc)CoOOH^{2+}$ can be prepared either electrochemically, by reduction of $(hmc)Co^{3+}$ in the presence of O_2 , or chemically, by adding an equivalent quantity of $Ru(NH_3)_6^{2+}$ to a solution of $(hmc)Co^{2+}$ in the presence of excess O_2 . The electrochemical oxidation of the product obtained from the chemical preparation is shown in Figure 6A. The voltammograms were recorded at the rotating disk electrode at the indicated times after the complex was prepared in solution. A single anodic wave is observed with a half-wave potential near 0.7 V. The anodic plateau current obtained 4 min after the solution was prepared is about 1.5 times as large as that for the oxidation of the same concentration of $(hmc)Co^{2+}$, as expected if the anodic wave resulted from the two-electron oxidation of $(hmc)CoOOH^{2+}$ according to half-reaction 5, but some of the



complex had decomposed to $(hmc)Co^{3+}$ and H_2O_2 before the plateau current could be measured. The oxidation wave in Figure 6A is better separated from the anodic background and its half-wave potential is ca. 0.2 V less positive than the ill-formed wave shown in curve 1 of Figure 3 for the oxidation at the glassy carbon ring of $(hmc)CoOOH^{2+}$ generated at the disk electrode. The position and shape of the current-potential curves for the oxidation of $(hmc)CoOOH^{2+}$ were sensitive to the pretreatment of the glassy carbon surface, and we attribute the less positive half-wave potential at the glassy carbon disk to the presence of more functional groups on the polished glassy carbon, which facilitates the oxidation.

The spontaneous decomposition of the $(hmc)CoOOH^{2+}$ complex was monitored by measuring the anodic plateau currents of curves such as those in Figure 6A as a function of time. A first-order process was observed with a rate constant of $9 \times 10^{-5} s^{-1}$ (Figure 6B). The cathodic voltammetry of a solution containing $(hmc)CoOOH^{2+}$ and $Ru(NH_3)_6^{3+}$ after O_2 was removed is shown in Figure 6C for solutions of varying ages. The first cathodic wave near 0.15 V corresponds to the reduction of $(hmc)Co^{3+}$ formed by the partial decomposition of $(hmc)CoOOH^{2+}$. The second cathodic wave near -0.15 V involves the reduction of both $(hmc)CoOOH^{2+}$ and the $Ru(NH_3)_6^{3+}$ formed during its preparation. The half-wave potentials for these two reductions are too close together to yield separate waves. As time passes, the plateau current of the first wave increases and that of the second wave decreases but the total cathodic current remains unchanged. This is the behavior expected as $(hmc)CoOOH^{2+}$ decomposes into $(hmc)Co^{3+}$ because both complexes are reduced in one-electron steps and their diffusion coefficients should be very similar.

Digital Simulations. To check the interpretations of the electrochemical responses that we have proposed, a commercially available digital simulation program^{16,17} was employed to calculate cyclic voltammograms for comparison with those obtained experimentally. The cyclic voltammetry for a solution of $(hmc)Co^{3+}$ in the absence of O_2 was used to determine the kinetic parameters for this simple, one-electron reaction. The parameters which produced the best agreement between the simulated and the experimental curves, shown in Figure 7A, are given in the figure caption.

(16) Rudolph, M.; Reddy, D. P.; Feldberg, S. W. *DigiSim 1.0 Software*; BioAnalytical Systems Inc.: West Lafayette, IN, 1993.

(17) Rudolph, M.; Reddy, D. P.; Feldberg, S. W. *Anal. Chem.* **1994**, *66*, 589A.

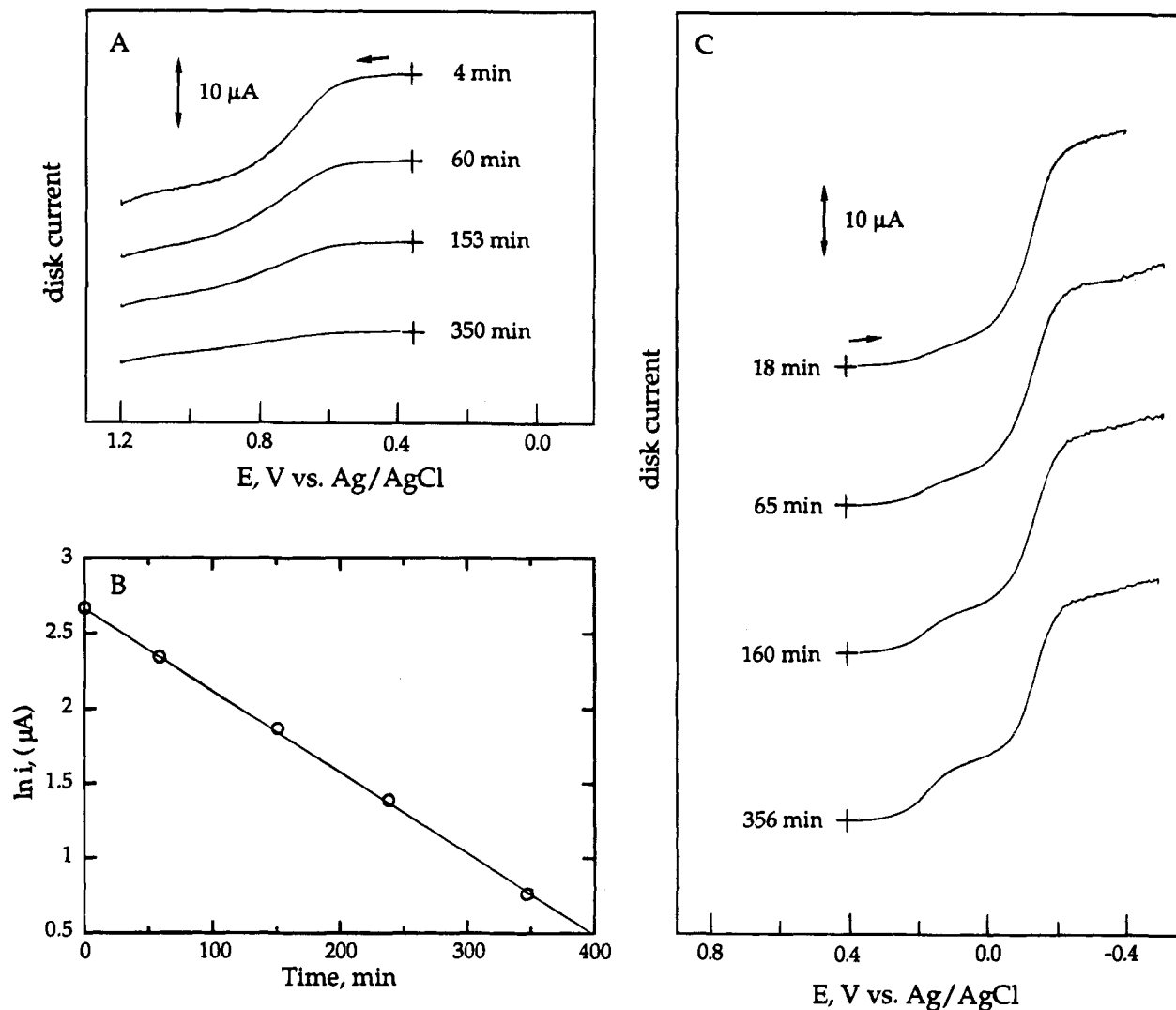


Figure 6. (A) Current-potential curves recorded with the rotating disk electrode in a solution prepared by adding an equimolar quantity of Ru(NH₃)₆²⁺ to a solution of (hmc)CoOO²⁺ generated as in Figure 5. The total cobalt concentration was 0.23 mM. The times elapsed since the solution was prepared are indicated. Rotation rate = 400 rpm. Other conditions were as in Figure 2. (B) First-order kinetic plot of anodic disk current for the oxidation of (hmc)CoOOH²⁺ vs the time elapsed since the complex was prepared. (C) Repeat of experiments similar to those in (A) except O₂ was removed from the solution and the potential scans were extended to -0.5 V.

The reduction of (hmc)Co³⁺ was then carried out in the presence of O₂, and the process was assumed to proceed by means of the three reactions given in Scheme 1. Because E_3^f is much more positive than E_2^f , changes in the kinetic parameters for reaction 3 had essentially no impact on the calculated cathodic voltammogram that is shown in Figure 7B along with the experimental curve. The parameters evaluated from Figure 7A were combined with the known kinetic parameters of reaction 1 to obtain the simulated curve. The agreement between the calculated and measured curves could be improved somewhat by using slightly different values of the rate constants for reaction 1 than those reported in ref 6 but the cathodic portion of the experimental curve is reasonably well accommodated by the mechanism of Scheme 1.

To obtain a simulated response for the anodic wave in Figure 7B, it was necessary to provide the program with the kinetic parameters corresponding to the individual steps involved in the anodic oxidation of (hmc)CoOOH²⁺. Scheme 1 operating in reverse was the assumed mechanism. The possibility that the (hmc)CoOO²⁺ complex, formed as an intermediate during the oxidation, could be oxidized without prior dissociation into (hmc)Co²⁺ and O₂ was not included in the mechanism because the (hmc)CoOO³⁺ complex that would result represents a high-

energy intermediate whose formation might well require even more positive potentials than those where the oxidation of (hmc)CoOOH²⁺ occurs. Thus, the simulation was carried out on the basis of Scheme 1 proceeding in the reverse direction with the formal potential and standard rate constant for half-reaction 3 adjusted to give the best agreement with the experimental voltammogram.

The oxidation of (hmc)CoOOH²⁺ prepared chemically in a solution containing no O₂ was also investigated. The experimental and simulated anodic voltammograms are shown in Figure 7C. The parameters used to obtain the simulated voltammogram are given in the figure caption. They are in satisfactory agreement with those used to fit the anodic wave in Figure 7B. The most interesting parameter to come out of the digital simulations was an approximate formal potential (at pH 1) for half-reaction 3 of ca. 0.77 V vs Ag/AgCl or 0.99 V vs NHE.

Discussion

A primary objective in carrying out this study was to try to evaluate the effect of the coordination to cobalt on the reactivities of dioxygen and its various reduction products. The formal potentials estimated for the [(hmc)CoOO²⁺ + H⁺]/(hmc)-

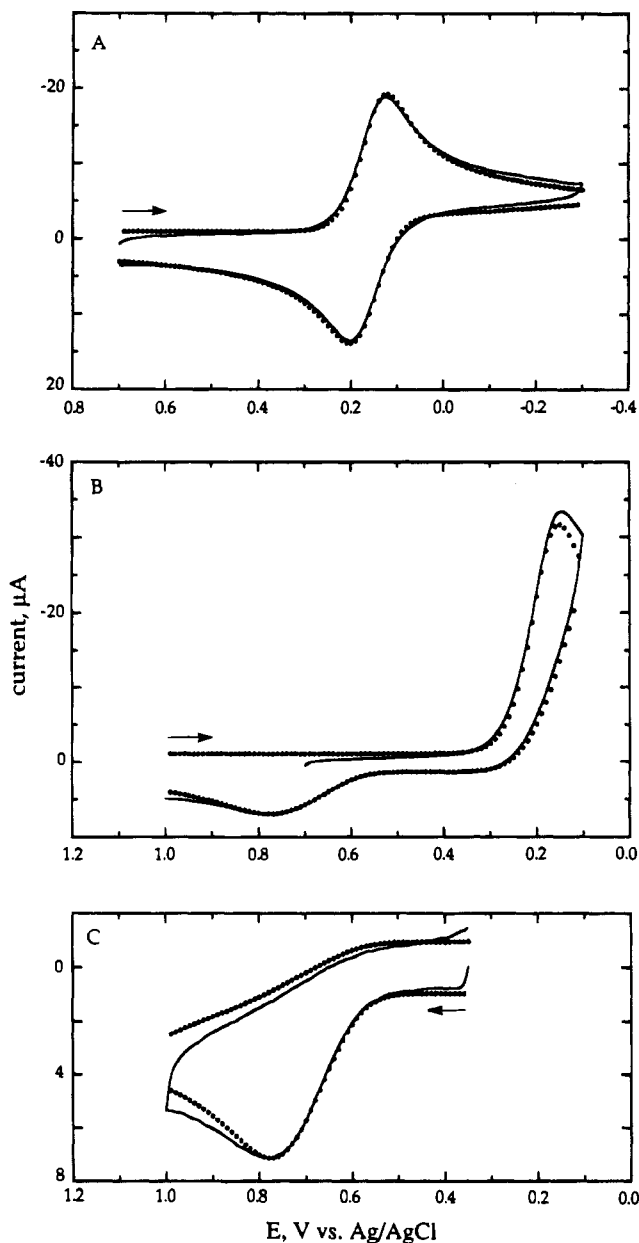
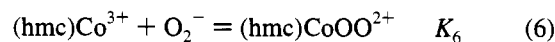


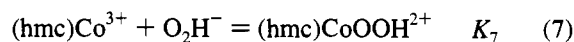
Figure 7. (A) Comparison of an experimental (solid line) with a simulated (dotted line) cyclic voltammogram for 0.63 mM (hmc)Co³⁺. The measured parameters used in the simulation were $E_2^f = 0.163$ V, scan rate = 50 mV s⁻¹, uncompensated resistance = 97 Ω, double-layer capacitance = 19 μF, electrode area = 0.248 cm², and diffusion coefficient of (hmc)Co³⁺ and (hmc)Co²⁺ = 3.9×10^{-6} cm² s⁻¹. The values of the heterogeneous rate constant, k_s , and transfer coefficient, α , adjusted to obtain the best agreement with the experimental voltammogram were $k_s = (6 \pm 2) \times 10^{-3}$ cm s⁻¹ and $\alpha = 0.76 \pm 0.04$. (B) Repeat of (A) but in the presence of 0.25 mM O₂. The simulated curve was based on Scheme 1 using the parameters from (A) for half-reaction 2, $k_1 = 5 \times 10^6$ M⁻¹ s⁻¹ and $K_1 = 3 \times 10^2$ M⁻¹ for reaction 1, and $E_3^f = 0.772 \pm 0.02$ V, $k_s = (2.5 \pm 0.5) \times 10^{-3}$ cm s⁻¹, and $\alpha = 0.67 \pm 0.03$ for half-reaction 3. (C) Experimental (solid line) and simulated (dotted line) voltammograms for the oxidation of 0.15 mM (hmc)CoOOH₂⁺ prepared as in Figure 6. The parameters used to obtain the simulated curve shown were as in (A) for half-reaction 2, as in (B) for reaction 1, and $E_3^f = 0.764 \pm 0.02$ V, $k_s = (3.0 \pm 0.5) \times 10^{-3}$ cm s⁻¹, and $\alpha = 0.64 \pm 0.02$ for half-reaction 3.

CoOOH₂⁺ and the [(hmc)Co³⁺ + O₂]/(hmc)CoOO₂²⁺ couples permit a few general comments on the chemistry involved. The (hmc)CoOO₂²⁺ complex can be regarded as an O₂ adduct of (hmc)Co²⁺ or as an O₂⁻ complex of (hmc)Co³⁺. As Taube has emphasized,¹⁸ a definitive distinction between the two

formulations is not meaningful. Nevertheless, the equilibrium constant for the hypothetical reaction between O₂⁻ and (hmc)Co³⁺, reaction 6, can be calculated from E_2^f , K_1 , and the



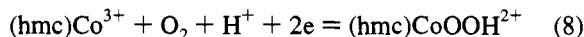
standard potential of the O₂/O₂⁻ couple (-0.16 V vs NHE with 1 M O₂ as standard state). The result is $K_6 = 4 \times 10^{11}$ M⁻¹. The formal potential at pH 1 for the reduction of (hmc)CoOO₂²⁺ to (hmc)CoOOH₂⁺ estimated in this study, $E_3^f = 0.99$ V (vs NHE) can be compared with that for the reduction of O₂⁻ to HO₂⁻ at pH 1 (0.97 V vs NHE). The close similarity of these potentials shows that O₂⁻ and O₂H⁻ have comparable affinities for (hmc)Co³⁺. The calculated value of the equilibrium constant for reaction 7 is $K_7 = 1 \times 10^{12}$ M⁻¹, reflecting the slightly



higher affinity of the O₂H⁻ ligand. As pointed out by Espenson *et al.*¹⁹ in comparing the equilibrium constants for the association of Cr³⁺ with the same two ligands, O₂H⁻ is a stronger base toward protons than is O₂⁻ by a factor of almost 10⁷, yet we find that O₂⁻ has almost as high an affinity for (hmc)Co³⁺ as does O₂H⁻. In ref 19 O₂H⁻ was calculated to exhibit weaker basicity toward Cr³⁺ than does O₂⁻, but when a corrected value for the formal potential of the CrOO₂²⁺/CrOOH₂⁺ couple⁵ is utilized in the calculation, the two ligands are found to have comparable equilibrium constants for association with Cr³⁺ just as they do for association with (hmc)Co³⁺. Taube¹⁸ has pointed out the unexpectedly strong association of O₂⁻ with Co(III) complexes and discussed the likelihood that greater ligand-to-metal charge transfer in complexes with O₂⁻ than in those with O₂H⁻ could produce comparable association constants for the two ligands despite their incomparable basicities toward protons. The same line of reasoning can be applied, although to a lesser extent, in the case of the corresponding pair of complexes of Cr³⁺ studied by Espenson *et al.*¹⁹ In line with the conclusion about the comparable affinities of O₂⁻ and O₂H⁻ for both (hmc)Co³⁺ and Cr³⁺ is the close similarity of the formal potential for the CrOO₂²⁺/CrOOH₂⁺ couple at pH 1 reported recently in ref 5 (0.97 V vs NHE) and the value for the (hmc)CoOO₂²⁺/(hmc)CoOOH₂⁺ couple obtained in this study (0.99 V).

The high affinity of both O₂⁻ and O₂H⁻ for (hmc)Co³⁺ ($K_6 = 4 \times 10^{11}$ M⁻¹, $K_7 = 1 \times 10^{12}$ M⁻¹) suggests that one reason that the electroreduction of O₂ to O₂H⁻ occurs at more positive potentials in the presence of (hmc)Co³⁺ than in its absence is the stabilization of the reduction products, O₂⁻ and O₂H⁻, by coordination to (hmc)Co³⁺.

The half-reaction potential for the two-electron reduction of O₂ in the presence of (hmc)Co³⁺, half-reaction 8, can be



calculated from K_1 , E_2^f , E_3^f , and pH = 1 as 0.68 V vs NHE or 0.47 V vs Ag/AgCl with [O₂] = 1 atm as the standard state. The potential where half-reaction 8 is observed to proceed under these conditions is near 0.16 V vs Ag/AgCl (Figure 2, curve 5). Thus, an overvoltage of ca. 0.3 V is required to reduce O₂ to O₂H⁻ coordinated to (hmc)Co³⁺. The reduction of O₂ to O₂H⁻ "coordinated" to H⁺ (i.e., the reduction of O₂ to H₂O₂) at graphite requires an overvoltage of about 1 V despite the slightly higher affinity of O₂H⁻ for H⁺ than for (hmc)Co³⁺.

(18) Taube, H. *Prog. Inorg. Chem.* **1986**, *34*, 607.

(19) Espenson, J. H.; Bakac, A.; Janni, J. *J. Am. Chem. Soc.* **1994**, *116*, 3436.

This large difference in the kinetics of the reduction of O₂ is a consequence of the fundamentally different mechanisms involved in the two cases. The participation of the intermediate (hmc)Co²⁺ complex in an inner-sphere reaction with O₂ provides a more facile reduction pathway than is available in the reduction of O₂ directly on the electrode surface in the absence of (hmc)Co³⁺.

The reduction of O₂ that can be achieved near 0.16 V (vs Ag/AgCl) in the presence of (hmc)Co³⁺ is not catalytic because the metal complex is trapped as (hmc)CoOOH²⁺ at this potential and when all of the complex is converted to (hmc)CoOOH²⁺ the reduction of O₂ ceases. The reduction of O₂ to H₂O₂ in the presence of (hmc)Co³⁺ is a catalytic process at potentials more negative than ca. -0.15 V (vs Ag/AgCl) corresponding to wave II in Figure 2. This potential is 0.2–0.3 V more positive than the potential where the reduction of O₂ to H₂O₂ proceeds at graphite electrodes in the absence of (hmc)Co³⁺, but it is determined by the potential for the reduction of the cobalt(III) center of (hmc)CoOOH²⁺, not by the potential of an "activated" Co–O₂ complex.

The formal potential for half-reaction 4 can be calculated from K₁, E₃^f, and the standard potential of the O₂/H₂O₂ couple. The result is E₄^f = 0.08 V vs Ag/AgCl at pH 1. The observed half-wave potential for wave II of Figure 2 is at -0.15 V vs Ag/AgCl. Thus, the high affinity of (hmc)Co³⁺ for O₂H⁻ causes an overvoltage of 0.23 V to be required for the reductive breaking of the cobalt(III)–O₂H⁻ bond. Such behavior, which is not uncommon in the electrochemistry of complexes of Co(III),²⁰ was also observed with the analogous (cyclam)-CoO₂H²⁺ complex.²

In the case of Cr³⁺, the (H₂O)₅CrOOH²⁺ complex was electroreducible to Cr(OH)₂³⁺ and H₂O so that the effect of the metal center on the reactivity as an oxidant of the coordinated O₂H⁻ could be inspected.⁵ Such a comparison was not possible with the (hmc)CoOOH²⁺ complex because the metal center is reduced before the coordinated ligand and H₂O₂ is released from the resulting, labile (hmc)CoOOH⁺ complex.

Espenson and co-workers recently described the kinetics of the homogeneous reactions of the (cyclam)CoOOH²⁺ and (hmc)CoOOH²⁺ complexes with several inorganic reductants.²¹ In most instances the coordinated O₂H⁻ ligand was reduced instead of, or before, the Co(III) center. The qualitative difference between the reactivity patterns exhibited by these Co(III) complexes in their chemical and electrochemical reductions reflects important mechanistic differences. The homogeneous reductions probably involve hydroperoxide-bridged transition states while the electrode surface, lacking functionalities suitable for bridging to hydroperoxide, delivers electrons more readily to the Co(III) center, which causes the coordinated hydroperoxide ligand to dissociate and escape reduction.

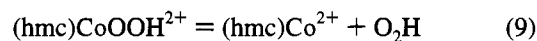
The oxidation of the O₂H⁻ ligand coordinated to (hmc)Co³⁺ occurs at potentials between 0.7 and 1.0 V vs Ag/AgCl depending on the state of the graphite surface (Figure 6A). H₂O₂ is not oxidized at graphite at these potentials so that the replacement of a proton in H₂O₂ by a (hmc)Co³⁺ center enhances the reactivity of the O₂H⁻ toward electrooxidation to O₂. The one-electron oxidation of (hmc)CoOOH²⁺ to (hmc)CoOO²⁺ is not observable because, at the potential where it could proceed (0.77 V vs Ag/AgCl), the (hmc)CoOO²⁺ produced would be rapidly further oxidized to (hmc)Co³⁺ and O₂ via the reverse of reaction 1 and half-reaction 2.

Table 2. Half-Reaction Potentials and Equilibrium Constants

reaction	E, V ^a vs NHE	note
(hmc)Co ³⁺ + e = (hmc)Co ²⁺	0.38	b
(hmc)Co ³⁺ + e + O ₂ = (hmc)CoOO ²⁺	0.36 (P _{O₂} = 1 atm; [O ₂] = 1.25 mM)	c
(hmc)CoOO ²⁺ + e + H ⁺ = (hmc)CoOOH ²⁺	0.53 ([O ₂] = 1 M)	d
(hmc)CoOOH ²⁺ + e + H ⁺ → (hmc)Co ²⁺ + H ₂ O ₂	0.30	c
(hmc)Co ³⁺ + O ₂ + H ⁺ + 2e → (hmc)CoOOH ²⁺	0.68 (P _{O₂} = 1 atm; [O ₂] = 1.25 mM)	c
	0.76 ([O ₂] = 1 M)	
reaction	equil const	note
(hmc)Co ²⁺ + O ₂ = (hmc)CoOO ²⁺	3 × 10 ² M ⁻¹	e
(hmc)Co ³⁺ + O ₂ ⁻ = (hmc)CoOO ²⁺	4 × 10 ¹¹ M ⁻¹	c
(hmc)Co ³⁺ + O ₂ H ⁻ = (hmc)CoOOH ²⁺	1 × 10 ¹² M ⁻¹	c

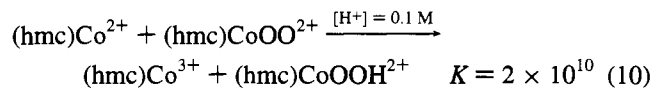
^a Potentials are for pH = 1 (0.1 M CF₃COOH). ^b Measured potential; reaction reversible. ^c Calculated values. ^d Estimated by digital simulation. ^e Measured by Espenson *et al.*⁶

The homolytic dissociation of the (hmc)CoOOH²⁺ complex in a reaction analogous to the reverse of reaction 1 would produce a good reductant and a very strong oxidant, reaction 9, that could undergo rapid outer-sphere electron transfer. The



net result would be the aquation of the (hmc)CoOOH²⁺ complex. The relative longevity of the (hmc)CoOOH²⁺ complex (Figure 6) indicates that reaction 9 must proceed very slowly if at all, a conclusion consistent with the equilibrium constant of 4 × 10⁻¹⁹ M that can be calculated for reaction 9 from E₂^f, E_{O₂H/O₂H⁻}^f,²² and K₇. By contrast, the homolytic dissociation of the (hmc)CoOO²⁺ complex proceeds at a much higher rate, k₁ = 1.6 × 10⁴ s⁻¹,⁶ and the electrooxidation of the resulting (hmc)Co²⁺ is readily observed (Figure 5). (The high substitutional lability of the (hmc)Co²⁺–O₂ system prevented us from establishing whether the electrooxidation of (hmc)CoOO²⁺ is preceded by its dissociation or if both the dissociated and undissociated complexes are oxidized in parallel.)

In Table 2 are collected the measured and calculated potentials for the various half-reactions that were investigated in this study. The rather positive value of the potential calculated for the (hmc)CoOO²⁺/(hmc)CoOOH²⁺ couple implies that (hmc)Co²⁺ should easily reduce (hmc)CoOO²⁺ to (hmc)CoOOH²⁺, reaction 10. However, this reaction must not proceed rapidly because



mixtures of (hmc)Co²⁺, O₂, and (hmc)CoOO²⁺, such as the one used to record Figure 5, persist for several minutes. If reaction 10 occurred rapidly, the anodic portion of the composite wave in Figure 5 would not be present because the only species that is electrooxidizable at potentials near 0.2 V is (hmc)Co²⁺. Thus, the reduction of (hmc)Co³⁺ to (hmc)CoOOH²⁺ in the presence of O₂ must occur entirely at the electrode surface without the participation of reaction 10 in the reduction of the CoOO²⁺ complex. The low rate of reaction 10 despite its significant driving force is probably the result of the same steric factors that impede the close approach of the two reactants and that produce the much lower rate of formation of the μ-peroxo complex when the cobalt centers are complexed by the hmc instead of the cyclam ligand.

(20) Maki, N.; Tanaka, N. In *Encyclopedia of Electrochemistry of the Elements*; Bard, A. J., Ed.; Marcel Dekker, Inc.: New York, 1975; Vol. III, pp 43–210.

(21) Wang, W.-D.; Bakac, A.; Espenson, J. H. Submitted for publication in *Inorg. Chem.*

The fact that the electroreduction of $(hmc)CoOO^{2+}$ to $(hmc)CoOOH^{2+}$ proceeds at potentials where the oxidation of $(hmc)Co^{2+}$ to $(hmc)Co^{3+}$ also occurs means that reaction 10 can be catalyzed at electrode surfaces at open circuit where the oxidation and reduction half-reactions can proceed remotely but simultaneously. The composite anodic-cathodic waves observed with mixtures of $(hmc)Co^{2+}$ and O_2 in Figure 5 was one result of this circumstance. Another was our observation that the rate of disappearance of Co(II) from mixtures of $(hmc)Co^{2+}$ and O_2 increased substantially when glassy carbon powder was added to the mixtures.

Conclusions

This study has shown that the electrochemical behavior of the $(hmc)Co^{3+/2+}-O_2$ system resembles that of the corresponding $(cyclam)Co^{3+/2+}-O_2$ system.² However, the diminished tendency for the formation of the μ -peroxo-bridged dimeric complex with the $(hmc)Co^{3+/2+}-O_2$ system allowed the half-reaction potentials of the monomeric complexes given in Table 2 to be measured or calculated from measured potentials. The $(hmc)Co^{3+}$ complex, like the $(cyclam)Co^{3+}$ and $(H_2O)_5Cr^{3+}$ complexes, exhibits a remarkably high affinity for O_2^- , which suggests substantial contribution from ligand-to-metal charge transfer in the complex. The stabilization of O_2^- that results from its coordination to $(hmc)Co^{3+}$ is suggested as the primary reason that the reduction of O_2 commences at much more positive potentials in the presence of this complex. Taube offered a similar argument in his discussion of equilibria involving dioxygen species and metal ions.¹⁸ A summary of relevant half-reaction potentials for the reduction of O_2 to O_2^-

Table 3. Effects of Coordination to Transition Metal Centers on Half-Reaction Potentials for the One-Electron Reduction of O_2

half-reaction	E, V^a vs	
	NHE	ref
$O_2 + e = O_2^-$	-0.16	22
$O_2 + H^+ + e = HOO$	0.12	22
$O_2 + Cr^{3+} + e = CrOO^{2+}$	0.27 ^b	19
$O_2 + (hmc)Co^{3+} + e = (hmc)CoOO^{2+}$	0.53 ^b	<i>c</i>
$O_2 + (cyclam)Co^{3+} + e = (cyclam)CoOO^{2+}$	0.65 ^d	2

^a Standard state is $[O_2] = 1 M$. ^b Supporting electrolyte: 0.1 M CF_3COOH . ^c This work. ^d Supporting electrolyte: 0.5 M $HClO_4$.

is given in Table 3. This compilation makes clear how substantial the stabilization of O_2^- by coordination to transition metal centers can be. Such stabilization of coordinated O_2^- may also account for our observation that O_2H^- coordinated to $(hmc)Co^{3+}$ is electrooxidized at potentials where H_2O_2 is not. The $(hmc)Co^{3+/2+}$ couple is a modestly active catalyst for the electroreduction of O_2 to H_2O_2 , but its much lower reactivity toward H_2O_2 and the relatively negative value of the formal potential of the $(hmc)Co^{3+/2+}$ couple make it unattractive as a catalyst for the (two-step) reduction of O_2 to H_2O .

Acknowledgment. This work was supported by the National Science Foundation. Helpful suggestions by Dr. Chunnian Shi are a pleasure to acknowledge. We are grateful to Prof. James H. Espenson for providing us with ref 21 prior to publication.

IC941370P

(22) Sawyer, D. T. *Oxygen Chemistry*; Oxford University Press, Inc.: New York, 1991; p 21.